Virology 402 (2010) 164–176

Contents lists available at ScienceDirect

Virology

journal homepage: www.elsevier.com/locate/yviro

Global analysis of modifications of the human BK virus structural proteins by LC-MS/MS

Chiung-Yao Fang [a,b,e], Hsiang-Ying Chen [a], Meilin Wang [c], Pei-Lain Chen [a,d], Chi-Fang Chang [a], Li-Sheng Chen [a], Cheng-Huang Shen [e], Wei-Chih Ou [d], Ming-Daw Tsai [f,g], Pang-Hung Hsu [f,*], Deching Chang [a,*]

[a] Institute of Molecular Biology, National Chung Cheng University, Chia-Yi, Taiwan
[b] Department of Chemistry and Biochemistry, National Chung Cheng University, Chia-Yi, Taiwan
[c] Department of Microbiology and Immunology, Chung Shan Medical University, Taichung, Taiwan
[d] Department of Medical Laboratory Science and Biotechnology, Central Taiwan University of Science and Technology, Taichung, Taiwan
[e] Department of Urology, Chia-Yi Christian Hospital, Chia-Yi, Taiwan
[f] Genomics Research Center, Academia Sinica, Taipei, Taiwan
[g] Institute of Biological Chemistry, Academia Sinica, Taipei, Taiwan

ARTICLE INFO

Article history:
Received 8 February 2010
Returned to author for revision 3 March 2010
Accepted 17 March 2010
Available online 9 April 2010

Keywords:
Polyomavirus
BK virus
Structural protein
Protein modification
LC-MS/MS

ABSTRACT

BK virus, a human polyomavirus, may cause nephritis and urological disorders in patients who have undergone renal transplantation. Little is known about the characteristics of the BK viral proteins. In the current study, BK viral proteins were characterized by immunoblotting and LC-MS/MS. The results revealed that BK virus is composed of three structural proteins, VP1, VP2, and VP3 and four cellular histones, H2A, H2B, H3, and H4. The major structural protein, VP1, can be divided into 16 subspecies by two-dimensional gel electrophoresis. Modifications of VP1, VP2, and VP3 were comprehensively identified by LC-MS/MS. The presence of acetylation, cysteinylation, carboxymethylation, carboxyethylation, formylation, methylation, methylthiolation, oxidation, dioxidation, and phosphorylation could be identified. This is the first report providing an analysis of the global modifications present on polyomavirus structural proteins. The identification of these modifications of VP1, VP2, and VP3 should facilitate an understanding of the physiology of BKV during its life cycle.

Introduction

Members of *Polyomaviridae* consist of non-enveloped virus particles containing a circular double-stranded DNA genome that is packaged using the host cellular histones. Polyomaviruses are widely distributed among vertebrates, including humans, monkeys, rabbits, rodents, and birds (Tooze, 1981). However, the host range of each virus is highly restricted. Up to the present, 16 polyomaviruses have been identified (Perez-Losada et al., 2006), including murine polyoma, simian virus 40 (SV40), and various human polyomaviruses. The human polyomaviruses include JC virus (JCV) and BK virus (BKV), KI polyomavirus, WU polyomavirus, and Merkel cell polyomavirus (Allander et al., 2007; Feng et al., 2008; Gaynor et al., 2007). The genomic organization of the human viruses is similar to all other polyomaviruses. Specifically, the genome encodes two early proteins, large T (LT) and small t (st), and four late proteins, agnoprotein, VP1, VP2, and VP3. The outer shell of the polyomavirus consists of 72 VP1 pentamers that are arranged as 12 penta-coordinated and 60 hexa-coordinated to form an icosahedral structure (Rayment et al., 1982). The protruding C-arms of the major capsid protein, VP1, allow flexible interaction with the neighboring pentamers (Liddington et al., 1991). VP2 and VP3 are the minor capsid proteins. VP3 is translated from the second in-frame initiation codon of VP2. Therefore, the amino acid sequence of VP3 is identical to the two-thirds of the C-terminal sequence of VP2. Previous studies have demonstrated that a single copy of the C-terminus of either VP2 or VP3 is able to form a hairpin-like structure, which is inserted into the cavity of the VP1 pentamers (Chen et al., 1998).

The presence of heterogeneity involving the polyoma and SV40 VP1 proteins has been previously analyzed by two-dimensional (2-D) electrophoresis (Bolen et al., 1981; Forstova et al., 1993; Haynes and Consigli, 1992; O'Farrell and Goodman, 1976). The VP1s of polyoma and SV40 can be divided into six subspecies (Bolen et al., 1981; O'Farrell and Goodman, 1976). The individual VP1 subspecies may have particular functions, such as receptor recognition (Bolen et al., 1981) and hemagglutination activity (Bolen and Consigli, 1979). Charge heterogeneity seems to indicate that various post-translational modifications (PTMs) might be present in polyomavirus VP1. Phosphorylation has been identified for polyoma VP1 (Haynes and Consigli, 1992; Li and Garcea, 1994; Li et al., 1995; Ponder et al., 1977; Tan and Sokol, 1972).

* Corresponding authors. P.H. Hsu is to be contacted at Genomics Research Center, Academia Sinica, 128 Academia Road, Section 2, Nankang, Taipei 115, Taiwan. Fax: +886 2 2789 8811. D. Chang, Institute of Molecular Biology, National Chung Cheng University, 168, University Rd., Min-Hsiung, Chia-Yi 621, Taiwan. Fax: +886 5 272 2871.
E-mail addresses: phsu@gate.sinica.edu.tw (P.-H. Hsu), biodcc@ccu.edu.tw (D. Chang).

0042-6822/$ – see front matter © 2010 Elsevier Inc. All rights reserved.
doi:10.1016/j.virol.2010.03.029

Furthermore, methylation (Burton and Consigli, 1996), hydroxylation (Ludlow and Consigli, 1989), sulfation (Ludlow and Consigli, 1987b), and acetylation (Bolen et al., 1981) have also been reported for polyoma VP1. However, most types of modification, as well as the specific amino acids on polyomavirus VP1 that are modified, have not been identified.

The characteristic differences between VP2 and VP3 in polyomavirus remain unknown. Although VP3 shares the same C-terminal amino acid sequence as VP2, the amount of VP2 and VP3 in the virion is not identical and neither are they evenly distributed. The necessity of VP2 or VP3 to the polyomavirus life cycle has been investigated (Gasparovic et al., 2006; Gharakhanian et al., 2003). VP2 of SV40 promotes viral binding to host cells (Daniels et al., 2006). Myristylation of a glycine in the N-terminal region of VP2 has been demonstrated (Schmidt et al., 1989; Streuli and Griffin, 1987). Virus lacking myristylation of the first glycine shows a distorted structure when examined by electron microscopy and there are also defects in the early events that occur during viral entry (Krauzewicz et al., 1990; Sahli et al., 1993). It has been hypothesized that VP3 undergoes oligomerization and is inserted into the ER membrane, where the viroporin formed by VP3 oligomerization promotes the transportation of viral genome out of the ER membrane (Daniels et al., 2006). Phosphorylation of minor capsid proteins, VP2 and VP3, has been studied in SV40 and polyoma (Ponder et al., 1977; Tan and Sokol, 1972). However, the biological functions of phosphorylation, together with which specific amino acid residues are phosphorylated in the minor structural proteins, are still not known.

Since the structural proteins have features that are needed for interaction with host cells during viral replication, the PTMs may be involved in generating diversity, complexity, and heterogeneity across the structural proteins, which will enable them to adapt to the various interactions that are needed. However, little is known about the characteristics of BK viral proteins in this context. In this study, the BK viral proteins were analyzed by immunoblotting and LC-MS/MS. The modifications of the structural proteins were then comprehensively identified by LC-MS/MS. The findings should provide significant information that will be further understanding of the replication of BKV.

Results

Identification of BK viral proteins

BKV was propagated in Vero cells and purified by CsCl gradient centrifugation. The morphology of the purified BKV was observed by electron microscopy (data not shown). The population of the purified BKV appeared to be homogeneous. The size of BKV was approximately 42 nm in diameter. The viral proteins were then separated by SDS-PAGE. Twelve protein bands were detected on the gel (Fig. 1A). Bands 1, 2, 3, 4, 6, and 8 were the major capsid protein, VP1, as demonstrated by immunoblotting (Fig. 1B, a) and LC-MS/MS (Table 1). Bands 1, 2, and 3 were believed to be VP1 aggregates due to incomplete reduction (Chen et al., 2001). Bands 6 and 8 were presumed to be the degraded products of VP1 (Friedmann, 1976; Ludlow and Consigli, 1987a). Band 8 was not detected by immunoblotting, which may be due to limited amount of this band that was present. However, it was identified by LC-MS/MS to have five VP1-matched peptides (Table 1). Bands 5 and 7 appeared to be VP2 and VP3, respectively, as demonstrated by immunoblotting (Fig. 1B, b) and LC-MS/MS (Table 1). Furthermore, bands 9, 10, 11, and 12 were identified as histones 3 (Fig. 1C, a), 2B (Fig. 1C, b), 2A (Fig. 1C, c), and 4 (Fig. 1C, d), respectively, as demonstrated by immunoblotting and LC-MS/MS (Table 1). Histone 1 was not detected in this study (Fig 1C, e).

Subspecies analysis of the BKV structural proteins

The structural proteins of BKV were further analyzed by 2-D gel electrophoresis. IPG strips of pH ranges 4–7 and 6–9 were employed to analyze the subspecies of BKV structural proteins. Results showed that 17 protein spots with molecular weights near 42 kDa were found in the gel with the pH 4–7 gradient (Fig. 2A). Western blotting showed that spots 1 to 16 reacted with anti-VP1 antiserum (Fig. 2B). Spots 1 to 16, except for spot 11, were further identified as VP1 polypeptide by LC-MS/MS (Table 2). The amount of spot 11 was too small to allow LC-MS/MS detection. The pI values of the 16 VP1 subspecies ranged between 6.1 and 6.7 (Fig. 2A). Spot 17 was identified as actin (Table 2). One protein spot (spot 18) was found in the gel with a pH gradient of 6 to 9 (Fig. 2C). The molecular weight of spot 18 was about 29 kDa with a pI of approximately 7.0. Spot 18 was further identified as the minor capsid protein, VP3, by immunoblotting (Fig. 2D) and LC-MS/MS (Table 2). VP2 was not detected by 2-D gel electrophoresis (Fig. 2), which may be due to the limited amount that was present.

Modification analysis of the BKV structural proteins

To identify modifications of the structural proteins of BKV, a mass nanoflow LC-MS/MS system with high resolution and high mass accuracy was employed. The structural proteins, VP1, VP2, and VP3, were separated by SDS-PAGE, then excised and subjected to enzyme digestion. To obtain the most comprehensive identification of the modifications present in the BKV structural proteins, digestions were performed using trypsin, chymotrypsin, and GluC to increase the sequence coverage. The various modifications present on the VP1, VP2, and VP3 were identified by LC-MS/MS as shown in Supplemental Tables 1–3 and summarized in Figs. 3–6 and in Tables 3 and 4. Representative MS/MS spectra for identification of various modifications on BKV structural proteins are shown in Fig. 3. A total of nine different types of modification were found in the VP1 as shown in Fig. 4 and Table 3. The modifications were detected on 56 amino acids across VP1. In the disordered region, Cys-10 was modified with methylation and dioxidation. Cys-10 is conserved in the VP1 of BKV, SV40, and polyoma. The Ser-80, Ser-133, and Ser-327 residues of BK VP1 were phosphorylated. Phosphorylation of threonine or tyrosine was not detected in VP1, VP2, or VP3. The phosphorylated Ser-80, Ser-133, and Ser-327 of VP1 are located in the BC loop, DE loop, and C-arm, respectively, as compared to SV40 VP1 (Fig. 4, Table 3). Oxidation and dioxidation were the most common modifications on VP1. Oxidation and dioxidation occurred at 26 amino acids, specifically Cys-10, Cys-255, Cys-268, Pro-21, Pro-345, Met-56, Met-85, Met-110, Met-126, Met-162, Met-167, Met-190, Met-322, Met-325, Met-347, Met-361, Phe-76, Phe-152, Phe-304, Phe-335, His-137, His-139, Tyr-173, Tyr-323, Tyr-350, and Trp-280. Sixteen amino acids were formylated, specifically Lys-19, Lys-360, Ser-71, Ser-80, Ser-133, Ser-148, Ser-187, Ser-274, Ser-295, Ser-303, Ser-307, Ser-327, Thr-171, Thr-184, Thr-272, and Thr-359. Carboxylmethylation and carboxylethylation were identified on 11 lysines, Lys-19, Lys-26, Lys-30, Lys-69, Lys-135, Lys-143, Lys-172, Lys-195, Lys-288, Lys-297, and Lys-353. Cysteinylation was detected on Cys-50, Cys-105, Cys-208, and Cys-268. Methylthiolation on Cys-50 was also detected. Although hydroxylation and acetylation have been reported in polyoma VP1 (Bolen et al., 1981; Ludlow and Consigli, 1989), these modifications were not found for BK VP1.

Most modifications of VP2 occurred in the VP2/3 common region (Figs. 5 and 6 and Table 4). Ser-92 and Trp-105 in the VP2 unique region were formylated and oxidized/dioxidized, respectively. Phosphorylation was identified for Ser-223, Ser-248, and Ser-254 of VP2. Myristylation of N-terminal glycine was not detected for BK VP2 in this study (Fig. 5 and Table 4). Oxidation and dioxidation were also the most common modifications identified in VP2, specifically Trp-105, Trp-153, Trp-166, Trp-202, Trp-293, Met-120, Met-229, Met-262, Met-294, Pro-174, Pro-227, His-242, His-245, Tyr-247, and Phe-275. Formylation was also found to occur on Ser-92, Ser-175, Ser-248, Ser-269, Ser-272, Thr-259, Thr-279, and Thr-304. Carboxymethylation of VP2 was identified on Lys-278.

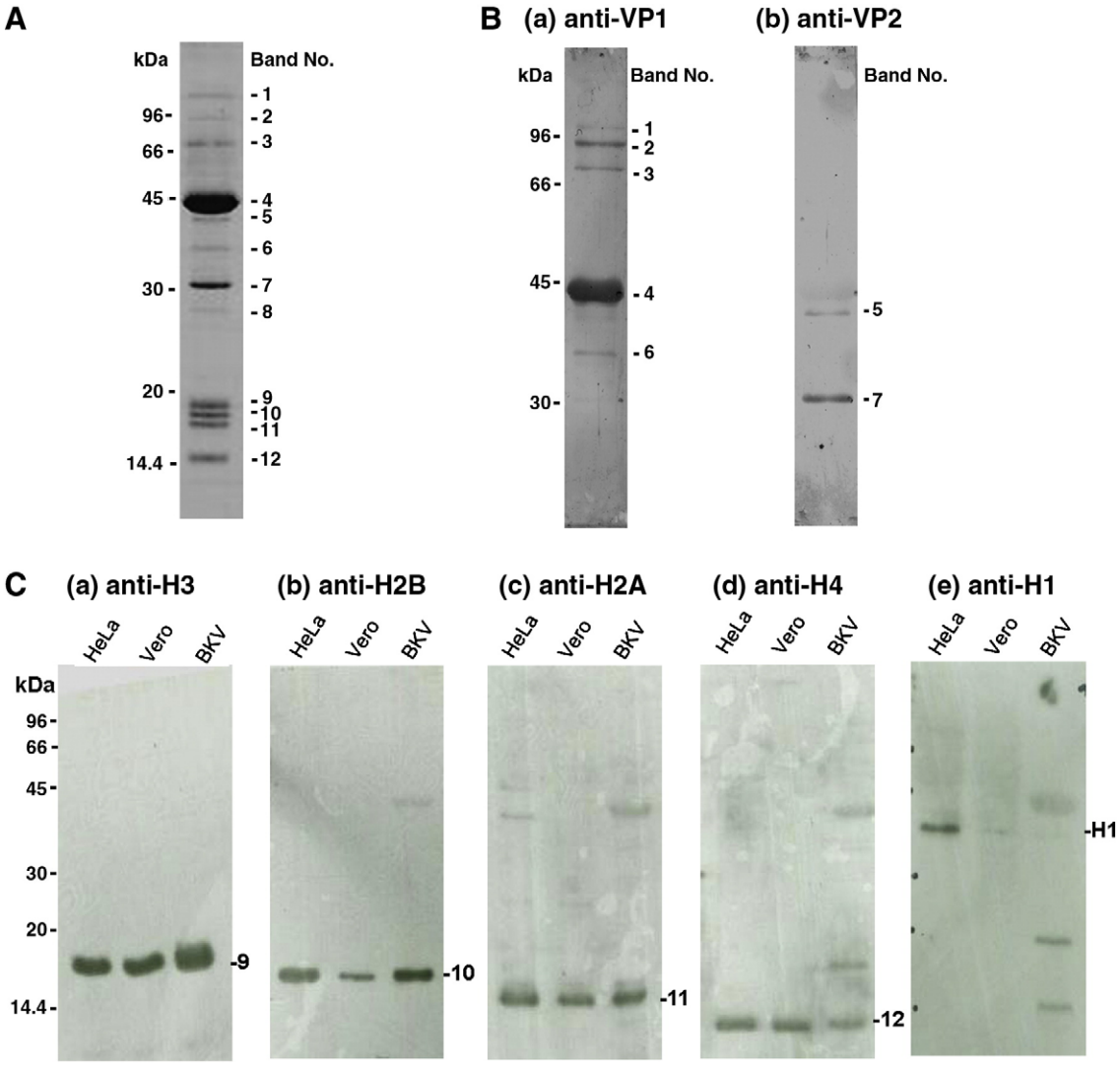

Fig. 1. Detection of BK viral proteins by SDS-PAGE and Western blot. (A) The BK viral proteins resolved by SDS-PAGE and stained by Coomassie blue. (B) Detection of (a) BK VP1 and (b) VP2/3. (C) Detection of BK (a) histone 3, (b) histone 2B, (c) histone 2A, (d) histone 4, and (e) histone 1. Histones from HeLa cells were used as controls. Vero cells were used as the host cells for the BK propagation. Band numbers are as referred to in (A).

Acetylation of the N-terminal methionine was identified for BK VP3 (Fig. 6). A single phosphorylation that occurred in VP3 Ser-129 was found and this corresponds to Ser-248 of VP2. Oxidation and dioxidation were also the most common modifications identified on VP3 (Fig. 6 and Table 4). Oxidation and dioxidation were identified on Met-110, Met-143, His-33, His-48, His-123, His-126, His-152, Trp-34, Trp-47, Trp-83, Asp-30, and Phe-156. Formylation was identified on Ser-56, Ser-129, Ser-135, Ser-150, Ser-153, Thr-84, and Thr-140. Carboxymethylation occurred on Lys-159 and Lys-200.

VP3 is translated from the second in-frame initiation codon of VP2. Therefore, the amino acid sequence of VP3 is identical to the two-thirds of the C-terminal sequence of VP2. However, some modifications between VP2 and VP3 are different. The initiation methionine was acetylated for VP3 but not for VP2 (Figs. 5 and 6 and Table 4). Phosphorylations were identified on three amino acids, Ser-223, Ser-248, and Ser-254 of VP2, but Ser-129, which corresponds to Ser-248 of VP2, was the only phosphorylated amino acid found for VP3. Lys-278 was the only amino acid carboxymethylated for VP2, but both Lys-159 (corresponding to Lys-278 on VP2) and Lys-200 (corresponding to Lys-319 on VP2) were carboxymethylated for VP3. Five amino acids, Asp-30, His-33, His-48, and His-152, modified by oxidation/dioxidation and four amino acids, Thr-84, Thr-170, Lys-200, and Lsy-220, modified by formylation or carboxylmethylation, were identified for VP3, whereas no modification of these amino acids was detected for VP2 (Table 4). Furthermore, five amino acids, Pro-174, Ser-223, Pro-227, Pro-291, and Pro-296, were found to be modified for VP2 but not for VP3.

Table 1
Identification of the BK viral proteins by SDS-PAGE and LC-MS/MS.

Band no.[a]	Protein[b]	Mol. mass (kDa)[c]	Sequence coverage (%)	Matched peptide
1	BK VP1	112.32	20	9
2	BK VP1	83.94	11	5
3	BK VP1	63.12	27	14
4	BK VP1	41.90	71	36
5	BK VP2	39.39	14	6
6	BK VP1	34.88	15	5
7	BK VP3	29.47	14	6
8	BK VP1	26.43	12	5
9	Histone 3	17.75	8	2
10	Histone 2B	17.16	19	2
11	Histone 2A	16.57	30	5
12	Histone 4	14.65	34	4

[a] Band numbers are the same as that in Fig. 1A.
[b] The tryptic peptides analyzed by mass spectrometry were matched with the amino acid sequences available on the NCBInr database.
[c] The molecular weights of BK viral proteins were estimated from SDS-PAGE.

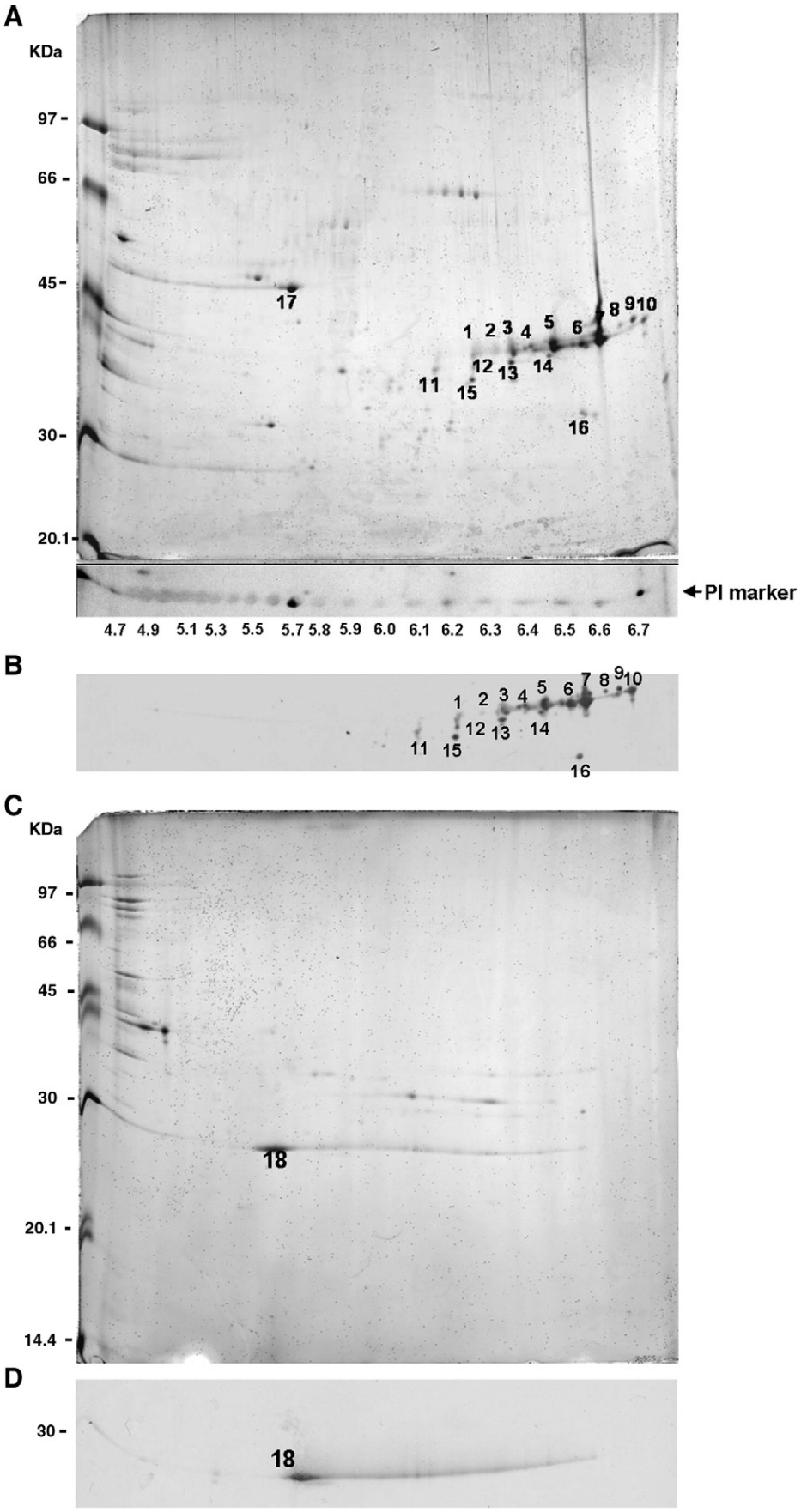

Fig. 2. Subspecies analysis of BK capsid proteins by two-dimensional gel electrophoresis. BKV was (A) resolved by 2-D gel electrophoresis with an immobilized pH 4–7 strip and stained with SyproRuby or (B) analyzed by Western blot using anti-BK VP1 antiserum. BKV was (C) resolved by 2-D gel electrophoresis with an immobilized pH 6–9 strip and stained with SyproRuby or (D) analyzed by Western blot using anti-BK VP2 antiserum.

Table 2
Subspecies identification of the BK structural proteins using 2-D gel electrophoresis followed by LC-MS/MS.

Spot no.[a]	Protein[b]	pI[c]	Sequence coverage (%)	Matched peptide	Percentage of total VP1 protein[d]
1	BK VP1	6.20	19	7	5.66
2	BK VP1	6.26	21	7	2.38
3	BK VP1	6.30	16	6	7.72
4	BK VP1	6.36	24	7	4.98
5	BK VP1	6.43	4	2	10.69
6	BK VP1	6.50	45	15	7.93
7	BK VP1	6.56	25	11	17.46
8	BK VP1	6.63	3	1	2.53
9	BK VP1	6.67	6	3	7.50
10	BK VP1	6.71	6	3	4.84
11	ND[e]	6.09	ND[e]	ND[e]	4.18
12	BK VP1	6.19	3	1	2.70
13	BK VP1	6.29	6	3	7.22
14	BK VP1	6.41	17	7	3.56
15	BK VP1	6.19	9	3	6.62
16	BK VP1'	6.50	6	2	4.04
17	Actin	5.61	11	3	–
18	BK VP3	ND	4	1	–

[a] Spot numbers are the same as that in Fig. 2.
[b] The tryptic peptides analyzed by LC-MS/MS were matched with the amino acid sequences available on the NCBInr database.
[c] Estimated pI values as compared with pI markers in Fig. 2A.
[d] The ratio of each VP1 subspecies was calculated from the volume of the individual spot divided by the sum of the total volume of 16 VP1 spots using the 2-D gel image and this was carried out by the Bio-Rad ImagQuant tool.
[e] Not determined.

Discussion

The viral proteins of human BKV were comprehensively analyzed in this study. BKV is composed of three structural proteins, VP1, VP2, and VP3, and four histones, H2A, H2B, H3, and H4. Histone 1 (H1) was not detected. The composition of BKV is similar to that of other polyomaviruses (Tooze, 1981). Furthermore, 16 subspecies of BK VP1 were detected by 2-D gel electrophoresis, immunoblotting, and LC-MS/MS. This is the first time that so many subspecies of polyomavirus VP1 have been identified. In addition, modifications of the structural proteins, VP1, VP2, and VP3, were also analyzed by LC-MS/MS. Cysteinylation, carboxymethylation, carboxyethylation, formylation, methylation, methylthiolation, oxidation, dioxidation, and phosphorylation were detected for VP1. Carboxymethylation, formylation, oxidation, dioxidation, and phosphorylation were identified for VP2. Acetylation, carboxymethylation, formylation, oxidation, dioxidation, and phosphorylation were identified for VP3. Some different modifications between VP2 and VP3 were also found although the amino acid sequence of VP3 is identical to that of two-thirds of VP2.

The 16 VP1 subspecies that were found on 2-D gel had pI values between 6.09 and 6.71 (Fig. 2 and Table 2). The heterogeneity of VP1 has been demonstrated in other polyomaviruses. Polyoma VP1 was found to have six subspecies with pI values between 5.75 and 6.75 (Bolen et al., 1981). SV40 VP1 can be divided into six subspecies with pI values ranging from pH 6.7 to pH 6.9 (O'Farrell and Goodman, 1976). In addition, a previous study demonstrated that BK VP1 is composed of four subspecies (Barbanti-Brodano et al., 1976).

Table 3
Summary of the modifications of BK VP1 as identified by LC-MS/MS.

a.a. no.	a.a. residue[a]	Modification[b]	Predicted structure[c]
10	C	methylation, dioxidation	disordered
19	K	formylation, carboxymethylation, carboxyethylation	N-arm
21	P	oxidation	N-arm
26	K	carboxymethylation	N-arm
30	K	carboxymethylation, carboxyethylation	β-A
50	C	methylthiolation, cysteinylation	β-B
56	M	oxidation, dioxidation	β-B
69	K	carboxymethylation	BC loop
71	S	formylation	BC loop
76	F	oxidation, dioxidation	BC loop
80	S	phosphorylation, formylation	BC loop
85	M	oxidation	BC loop
105	C	cysteinylation	CD
110	M	oxidation	β-D
126	M	oxidation, dioxidation	α-B
133	S	phosphorylation, formylation	DE loop
135	K	carboxymethylation	DE loop
137	H	oxidation	DE loop
139	H	oxidation	DE loop
143	K	carboxyethylation	DE loop
148	S	formylation	β-E
152	F	dioxidation	β-E
162	M	oxidation, dioxidation	EF loop
167	M	oxidation, dioxidation	EF loop
171	T	formylation	EF loop
172	K	carboxymethylation, carboxyethylation	EF loop
173	Y	oxidation	EF loop
184	T	formylation	EF loop
187	S	formylation	EF loop
190	M	oxidation, dioxidation	EF loop
195	K	carboxymethylation, carboxyethylation	EF loop
208	C	cysteinylation	EF loop
255	C	dioxidation	GH loop
268	C	dioxidation, methythiolation, cysteinylation	HI loop
272	T	formylation	HI loop
274	S	formylation	HI loop
280	W	oxidation, dioxidation	β-I
288	K	carboxymethylation	β-I
295	S	formylation	–
297	K	carboxymethylation, carboxyethylation	–
303	S	formylation	α-C
304	F	oxidation	α-C
307	S	formylation	α-C
322	M	oxidation, dioxidation	C-arm
323	Y	oxidation, dioxidation	C-arm
325	M	oxidation, dioxidation	C-arm
327	S	phosphorylation, formylation	C-arm
335	F	oxidation, dioxidation	β-J
345	P	oxidation	C-arm
346	D	methylthiolation	C-arm
347	M	oxidation, dioxidation	C-loop
350	Y	oxidation	C-loop
353	K	carboxymethylation, carboxyethylation	C-loop
359	T	formylation	C-loop
360	K	formylation	C-loop
361	M	oxidation, dioxidation	C-loop

[a] Abbreviation of the amino acid.
[b] Modification identified by LC-MS/MS.
[c] The tertiary structure was predicted according to that published for SV40 VP1 (32).

Fig. 3. Representative MS/MS spectra for identification of modifications on BKV structural proteins. (A) Cysteine methylation. Methylated Cys10 of VP1 was demonstrated by a trypsin-digested peptide KGEC$_{Me}$PGAAPK with a doubly charged precursor ion at 486.2522 (m/z). (B) Lysine carboxyethylation. Carboxyethylation of Lys30 of VP1 was found by a trypsin-digested peptide IK$_{carb\text{-}Et}$GGVEVLEVK with a doubly charged precursor ion at 621.8701 (m/z). (C) Lysine carboxymethylation. Carboxymethylated Lys30 of VP1 was demonstrated by a trypsin-digested peptide IK$_{carb\text{-}Me}$GGVEVLEVK with a doubly charged precursor ion at 614.8621 (m/z). (D) Serine formylation. Ser80 of VP1 with formylation was distinguished by a trypsin-digested peptide LSAENDFSSDS$_{formyl}$PERK with a doubly charged precursor ion at 855.3860 (m/z). (E) Serine phosphorylation. Phosphorylation of Ser80 of VP1 was identified by a trypsin-digested peptide LSAENDFSSDS$_{phos}$PERK with a doubly charged precursor ion at 881.3715 (m/z). (F) Methionine oxidation. Oxidated Met190 of VP1 was characterized by a trypsin-digested peptide NPTAQSQVM$_{ox}$NTDHK with a doubly charged precursor ion at 793.8649 (m/z). (G) Methionine dioxidation. Dioxidation of Met190 of VP1 was found by a trypsin-digested peptide NPTAQSQVM$_{di\text{-}ox}$NTDHK with a doubly charged precursor ion at 801.8646 (m/z). (H) Cysteine cysteinylation. Cysteinylation of Cys208 of VP1 was identified by a trypsin/chymotrypsin-digested peptide NNAYPVEC$_{cysteinyl}$WVPDPSR with a doubly charged precursor ion at 933.3959 (m/z). (I) Cysteine methylthiolation. Methylthiolation of Cys268 of VP1 was characterized by a trypsin/GluC-digested peptide ADSLYVSAADIC$_{Me\text{-}Thio}$GLFTNSSGTQQQWR with a triply charged precursor ion at 912.7558 (m/z). (J) N-terminal acetylation of VP3 was demonstrated by a doubly charged trypsin/chymotrypsin-digested peptide Ac-A LELFNPDEYY with the precursor ion at 708.3229 (m/z).

Different subspecies of VP1 may have different functions in the life cycle of the polyomavirus. Changes in VP1 heterogeneity seem to have an effect on plaque size; this has been demonstrated for SV40 (Barban, 1973) and polyoma (Hewick et al., 1977). Three out of six of the VP1 subspecies of polyoma were detected in capsomere preparations that had been enriched for hexon subunits (Bolen et al., 1981). Polyoma

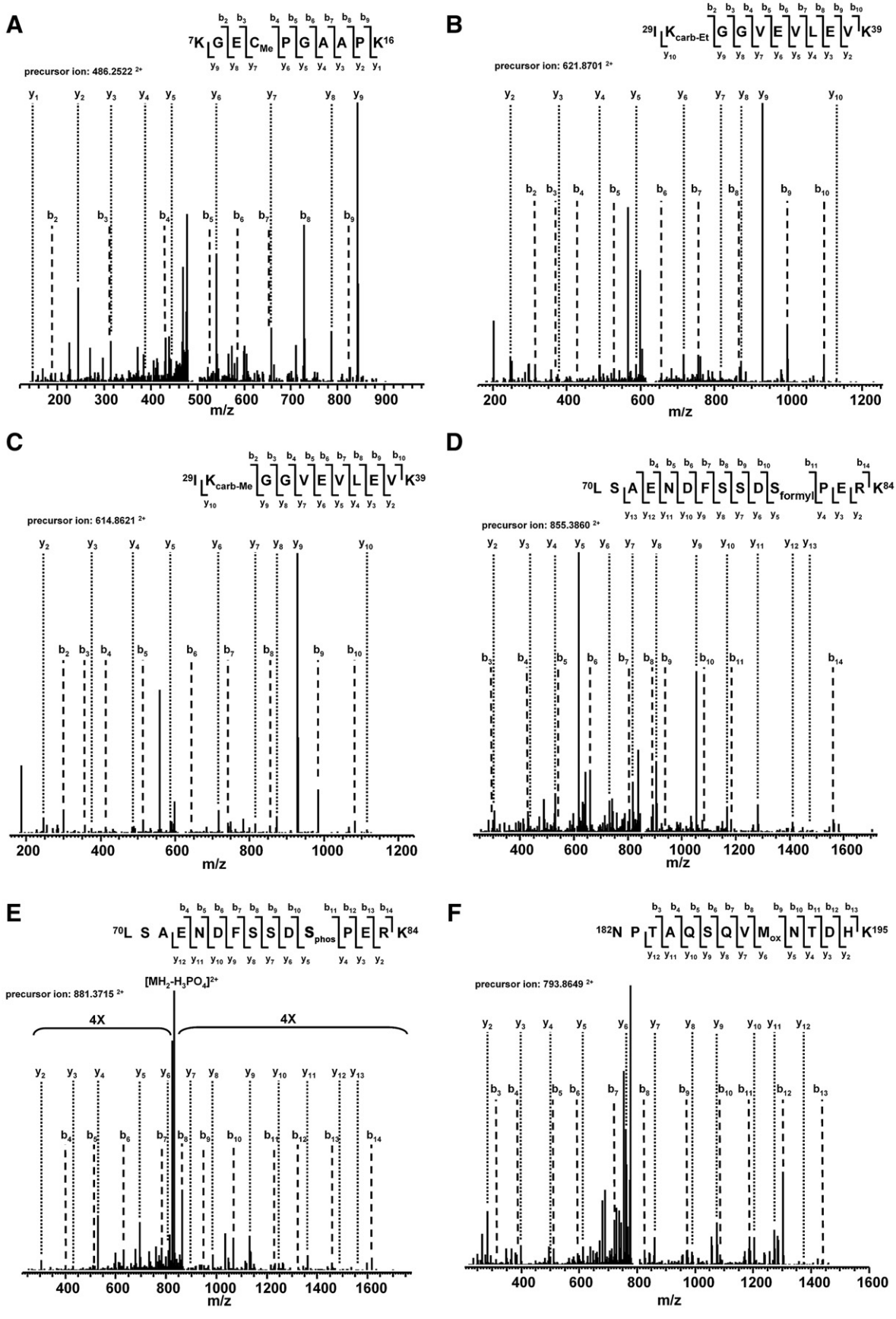

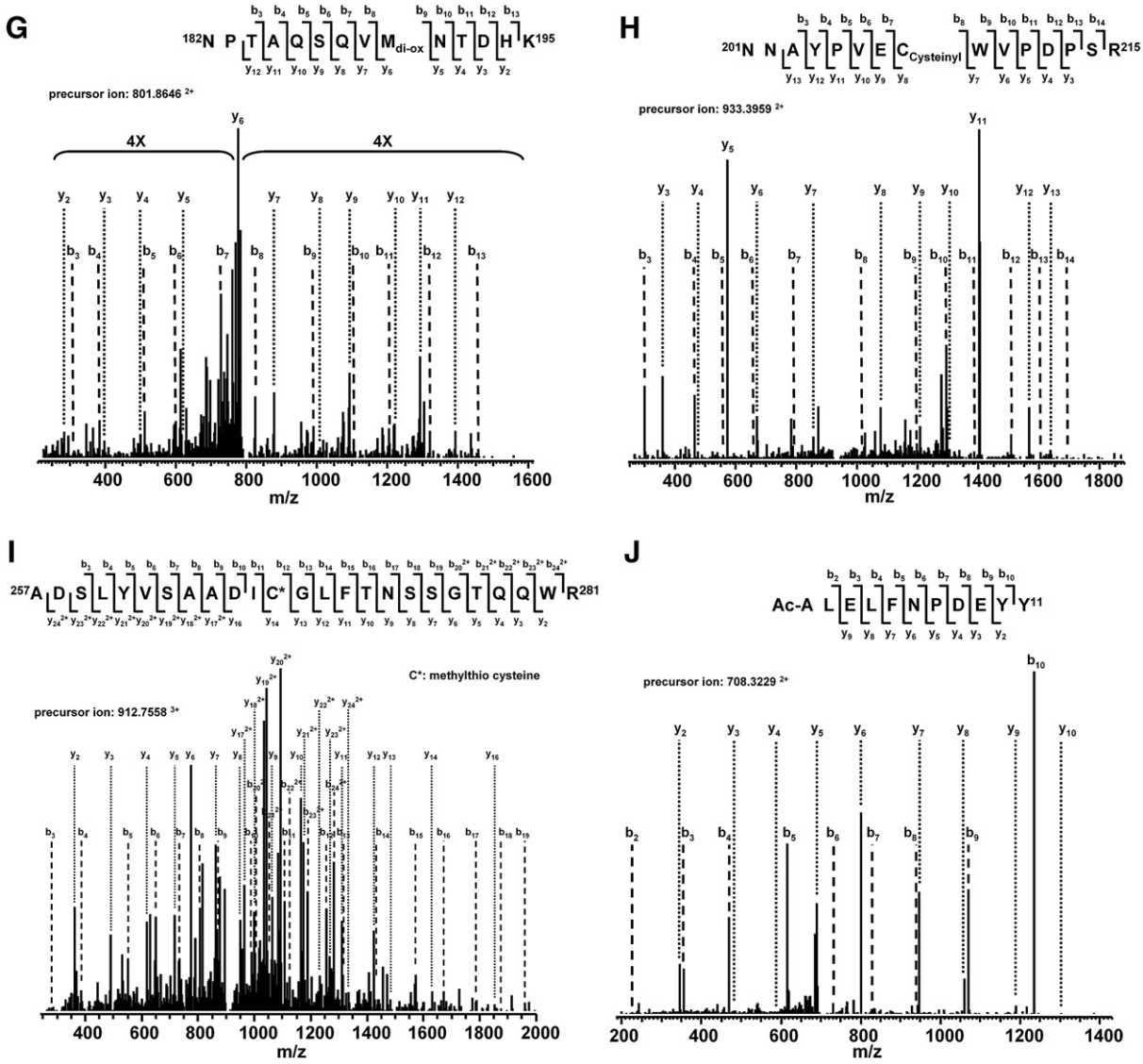

Fig. 3 (*continued*).

VP1 capsid with two subspecies missing fails to bind to the surface of mouse kidney cells (Bolen and Consigli, 1979). Taken together, it would seem that modifications of VP1 might play roles in the life cycle of the various polyomavirus. Subspecies of the minor capsid proteins, VP2 and VP3, of polyoma have also been analyzed (Bolen et al., 1981). VP2 has a pI of approximately pH 5.5 in both the virion and capsid. The pIs of VP3 in virion and capsid were found to be pH 7.0 and 6.5, respectively. In this study, BK VP2 was not detectable on our 2-D gel system and only one BK VP3 species with tailing was identified.

Recombinant VP1 expressed in *E. coli* is able to self-assemble to form a capsid-like structure (Ou et al., 1999; Salunke et al., 1986). Therefore, the PTM of VP1 appears not to be crucial for capsid formation (Salunke et al., 1986); however, under-phosphorylation of VP1 does produce a slight defect in virion assembly (Li et al., 1995), which reduces transforming activity (Garcea et al., 1985); this was demonstrated in polyoma. Ser-80, Ser-133, and Ser-327 of BK VP1 were identified as phosphorylated using LC-MS/MS in this study. When compared to other polyomavirus VP1 sequences, Ser-80 is conserved in BK, JC, SV40, and polyoma VP1 but Ser-133 and Ser-327 are not (Fig. 4). Nevertheless, phosphorylation of Thr-63, Ser-66, and Thr-156 of polyoma VP1 has been demonstrated (Li and Garcea, 1994; Li et al., 1995). None of these three phosphorylated amino acids is conserved in other polyomavirus VP1 (Fig. 4). It is not clear whether the differences in phosphorylation might result in different properties across the polyomaviruses. Ser-80, Ser-133, and Ser-327 of BK VP1 are located on BC loop, DE loop, and C-arm, respectively, as compared with SV40 VP1 (Liddington et al., 1991). BC and DE loops are at the surface of the capsid particle and may interact with cellular receptors (Stehle et al., 1994). As reported previously, the empty capsid lacking phosphorylated species from polyoma VP1 shows limited virion infection with permissive cells, although the protein's hemagglutination activity was retained (Anders and Consigli, 1983; Bolen et al., 1981; Bolen and Consigli, 1979). Therefore, it is possible that phosphorylation of the amino acids at the surface of the capsid particle will affect receptor binding. The polymorphism of the major capsid protein VP1 demonstrated here, especially in the outer BC, DE, and HI loops, of human polyomaviruses, JC and BK, seems to be associated with progression of the viral diseases (Boldorini et al.,

Fig. 4. Symbolic figure representing the modifications identified in BK VP1 (GenBank accession no. DQ305492). The VP1 amino acid sequences of JC (GenBank accession no. J02226), SV40 (GenBank accession no. J02400.1), and polyoma (GenBank accession no. U27813.1) were aligned with the BK VP1 sequence using SDSC Biology Workbench (San Diego Supercomputing Center, University of Illinois Host Biology Workbench) for this comparison. The tertiary structure referred to is that of SV40 VP1 (32).

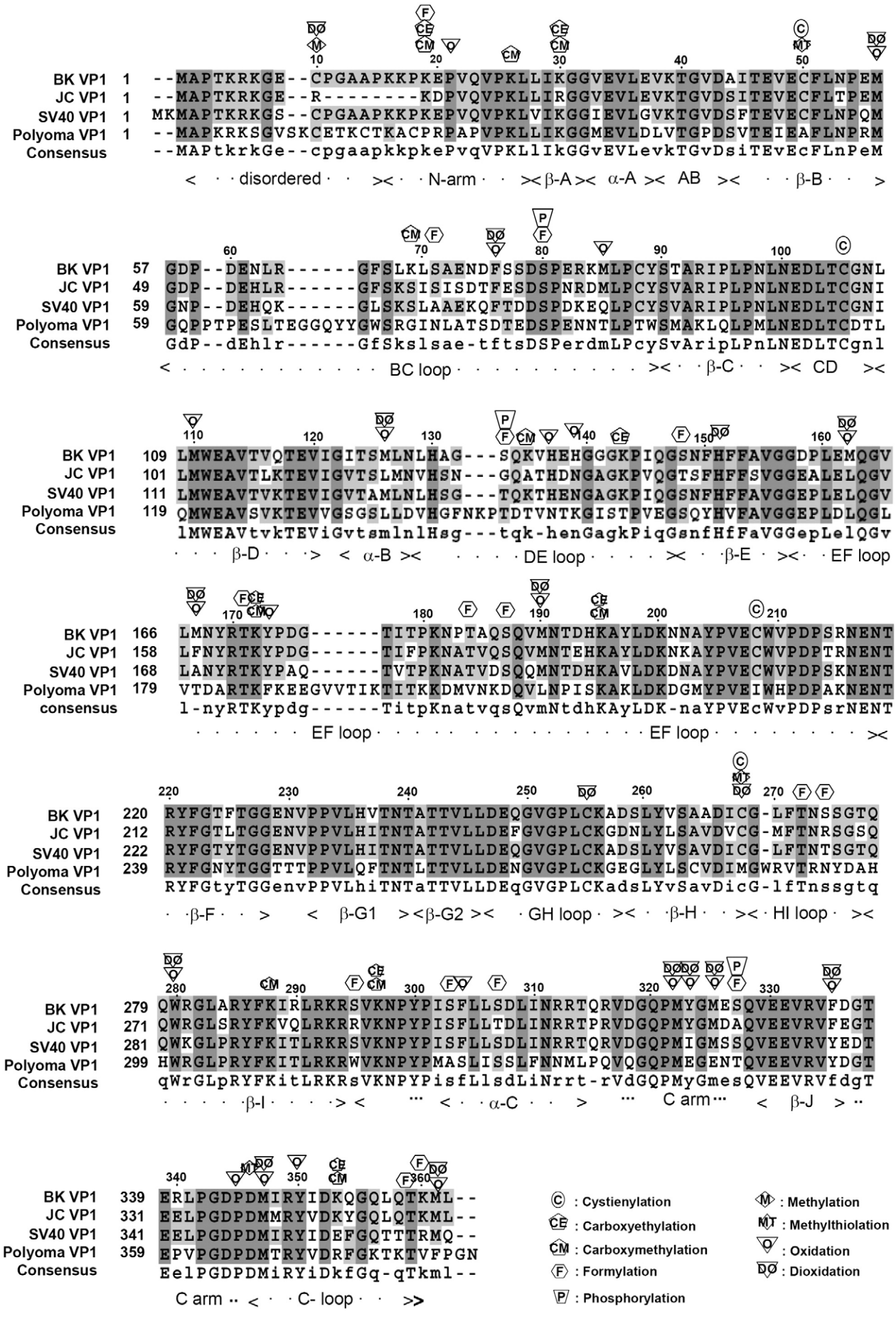
BK VP1 1 --MAPTKRKGE--CPGAAPKKPKEPVQVPKLLIKGGVEVLEVKTGVDAITEVECFLNPEM
JC VP1 1 --MAPTKRKGE--R---------KDPVQVPKLLIRGGVEVLEVKTGVDSITEVECFLTPEM
SV40 VP1 1 MKMAPTKRKGS--CPGAAPKKPKEPVQVPKLVIKGGIEVLGVKTGVDSFTEVECFLNPQM
Polyoma VP1 1 --MAPKRKSGVSKCETKCTKACPRPAPVPKLLIKGGMEVLDLVTGPDSVTEIEAFLNPRM
Consensus --MAPtkrkGe--cpgaapkkpkePvqVPKLlIkGGvEVLevkTGvDsiTEvEcFLnPeM
< · · disordered · · >< · · N-arm · · ><β-A>< α-A >< AB >< · · β-B · · >
BK VP1 57 GDP--DENLR------GFSLKLSAENDFSSDSPERKMLPCYSTARIPLPNLNEDLTCGNL
JC VP1 49 GDP--DEHLR------GFSKSISISDTFESDSPNRDMLPCYSVARIPLPNLNEDLTCGNI
SV40 VP1 59 GNP--DEHQK------GLSKSLAAEKQFTDDSPDKEQLPCYSVARIPLPNLNEDLTCGNI
Polyoma VP1 59 GQPPTPESLTEGGQYYGWSRGINLATSDTEDSPENNTLPTWSMAKLQLPMLNEDLTCDTL
Consensus GdP--dEhlr------GfSkslsae-tftsDSPerdmLPcySvAripLPnLNEDLTCgnl
< · · · · · · · · · · · · BC loop · · · · · · · · · · · · >< · · β-C · · >< CD ><
BK VP1 109 LMWEAVTVQTEVIGITSMLNLHAG---SQKVHEHGGGKPIQGSNFHFFAVGGDPLEMQGV
JC VP1 101 LMWEAVTLKTEVIGVTSLMNVHSN---GQATHDNGAGKPVQGTSFHFFSVGGEALELQGV
SV40 VP1 111 LMWEAVTVKTEVIGVTAMLNLHSG---TQKTHENGAGKPIQGSNFHFFAVGGEPLELQGV
Polyoma VP1 119 QMWEAVSVKTEVVGSGSLLDVHGFNKPTDTVNTKGISTPVEGSQYHVFAVGGEPLDLQGL
Consensus lMWEAVtvkTEViGvtsmlnlHsg---tqk-henGagkPiqGsnfHfFaVGGepLelQGv
· · · β-D · · >< α-B >< · · · · DE loop · · · · >< · β-E · >< · EF loop
BK VP1 166 LMNYRTKYPDG------TITPKNPTAQSQVMNTDHKAYLDKNNAYPVECWVPDPSRNENT
JC VP1 158 LFNYRTKYPDG------TIFPKNATVQSQVMNTEHKAYLDKNKAYPVECWVPDPTRNENT
SV40 VP1 168 LANYRTKYPAQ------TVTPKNATVDSQQMNTDHKAVLDKDNAYPVECWVPDPSKNENT
Polyoma VP1 179 VTDARTKFKEEGVVTIKTITKKDMVNKDQVLNPISKAKLDKDGMYPVEIWHPDPAKNENT
consensus l-nyRTKypdg------TitpKnatvqsQvmNtdhKAyLDK-naYPVEcWvPDPsrNENT
· · · · · · EF loop · · · · · · · · · · · · · · · · EF loop · · · · · · · · >
BK VP1 220 RYFGTFTGGENVPPVLHVTNTATTVLLDEQGVGPLCKADSLYVSAADICG-LFTNSSGTQ
JC VP1 212 RYFGTLTGGENVPPVLHITNTATTVLLDEFGVGPLCKGDNLYLSAVDVCG-MFTNRSGSQ
SV40 VP1 222 RYFGTYTGGENVPPVLHITNTATTVLLDEQGVGPLCKADSLYVSAVDICG-LFTNTSGTQ
Polyoma VP1 239 RYFGNYTGGTTPPVLQFTNTLTTVLLDENGVGPLCKGEGLYLSCVDIMGWRVTRNYDAH
Consensus RYFGtyTGGenvPPVLhiTNTaTTVLLDEqGVGPLCKadsLYvSavDicG-lfTnssgtq
· · β-F · · > < β-G1 ><β-G2 >< · GH loop · >< · · β-H · · >< · HI loop · ><
BK VP1 279 QWRGLARYFKIRLRKRSVKNPYPISFLLSDLINRRTQRVDGQPMYGMESQVEEVRVFDGT
JC VP1 271 QWRGLSRYFKVQLRKRRVKNPYPISFLLTDLINRRTPRVDGQPMYGMDAQVEEVRVFEGT
SV40 VP1 281 QWKGLPRYFKITLRKRSVKNPYPISFLLSDLINRRTQRVDGQPMIGMSSQVEEVRVYEDT
Polyoma VP1 299 HWRGLPRYFKITLRKRWVKNPYPMASLISSLFNNMLPQVQGQPMEGENTQVEEVRVYDGT
Consensus qWrGLpRYFKitLRKRsVKNPYPisfLlsdLiNrrt-rVdGQPMyGmesQVEEVRVfdgT
· · · · · β-I · · · · > < ··· < · · α-C · · > ··· C arm ··· < β-J > ··
BK VP1 339 ERLPGDPDMIRYIDKQGQLQTKML--
JC VP1 331 EELPGDPDMMRYVDKYGQLQTKML--
SV40 VP1 341 EELPGDPDMIRYIDEFGQTTTRMQ--
Polyoma VP1 359 EPVPGDPDMTRYVDRFGKTKTVFPGN
Consensus EelPGDPDMiRYiDkfGq-qTkml--
C arm ·· < · · C- loop · · >>
Ⓒ : Cystienylation
CE : Carboxyethylation
CM : Carboxymethylation
Ⓕ : Formylation
Ⓟ : Phosphorylation
Ⓜ : Methylation
MT : Methylthiolation
Ø : Oxidation
ØØ : Dioxidation

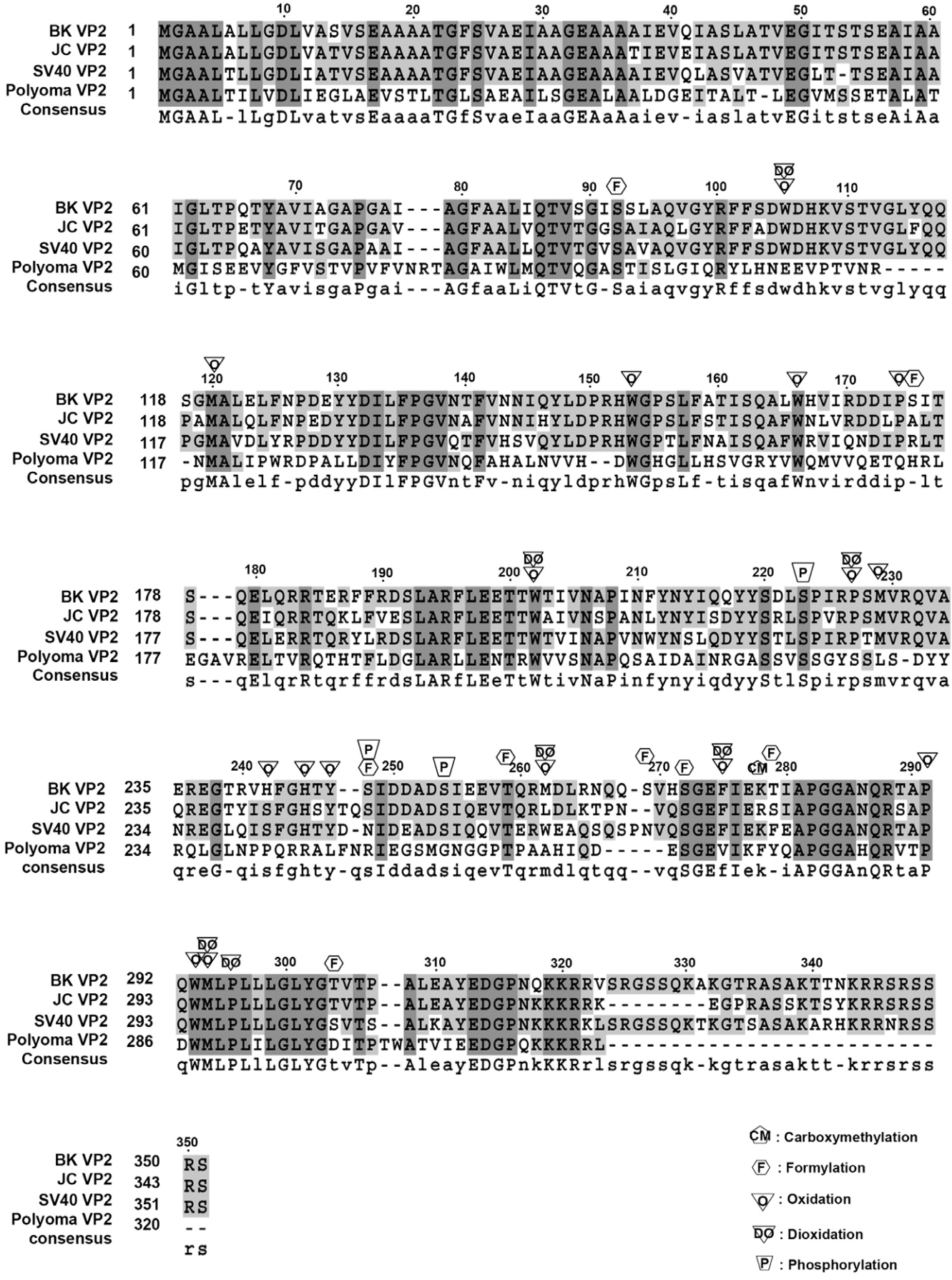

Fig. 5. Symbolic figure representation of the modifications identified in BK VP2 (GenBank accession no. DQ305492). The VP2 amino acid sequences of JC (GenBank accession no. J02226), SV40 (GenBank accession no. J02400.1), and polyoma (GenBank accession no. U27813.1) were aligned with the BK VP2 sequence using SDSC workbench for this comparison.

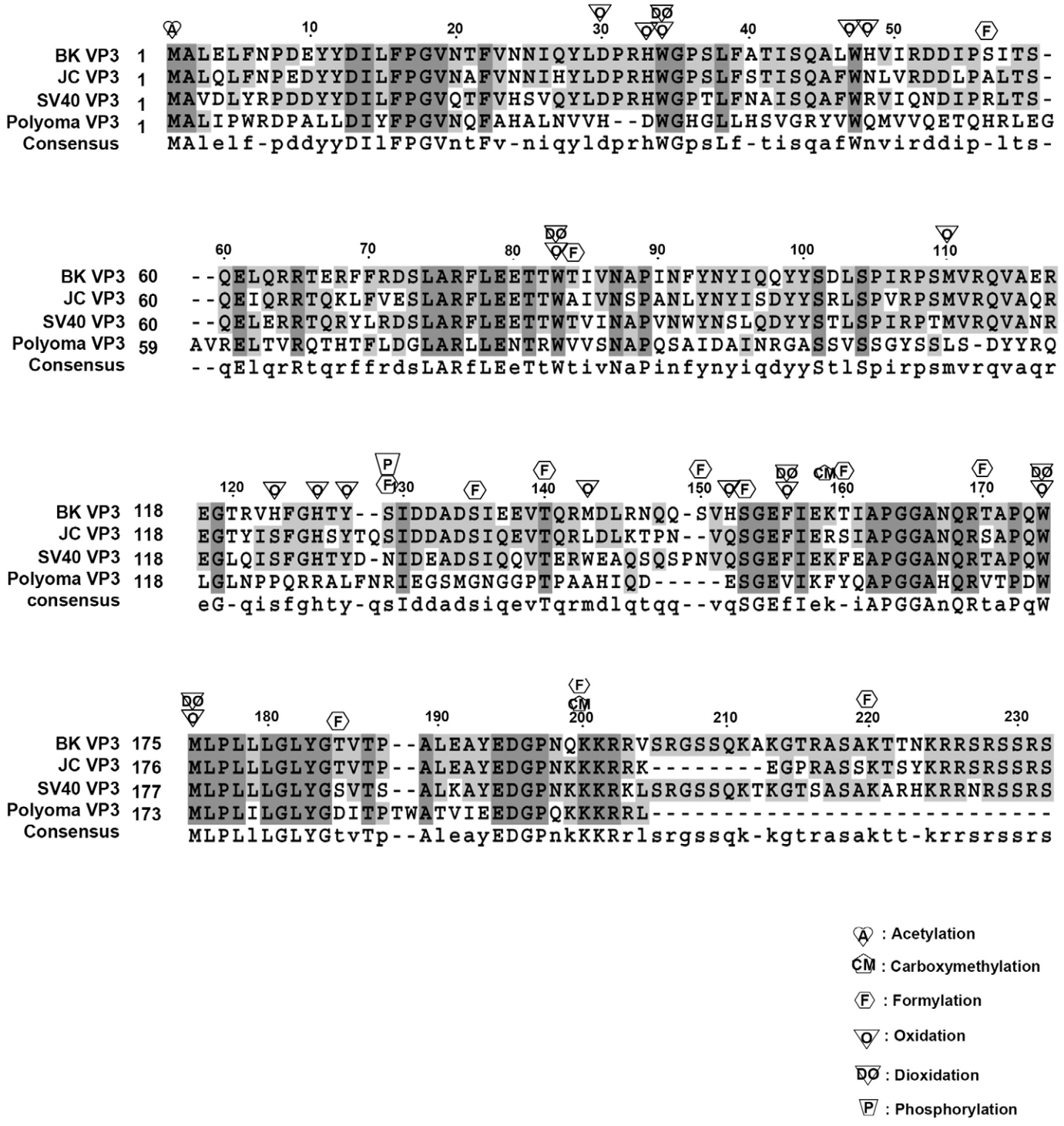

Fig. 6. Symbolic figure representation of the modifications identified in BK VP3 (GenBank accession no. DQ305492). The VP3 amino acid sequences of JC (GenBank accession no. J02226), SV40 (GenBank accession no. J02400.1), and polyoma (GenBank accession no. U27813.1) were aligned with the BK VP3 sequence using SDSC Biology Workbench (San Diego Supercomputing Center) for this comparison.

2009; Iida et al., 1993; Zheng et al., 2005). In the current study, the results also showed extensive modifications in the outer loops, and determining whether some of these modified amino acids are polymorphic will be important.

Ser-223, Ser-248, and Ser-254 of BK VP2 were phosphorylated. Ser-223 is conserved in BK, JC, SV40, and polyoma VP2. Ser-248 is conserved in BK and JC VP2. Ser-254 is conserved in BK, JC, and SV40 VP2 (Fig. 5). Ser-129, corresponding to Ser-248 of VP2, of VP3 is the only amino acid phosphorylated (Fig. 6). The C-terminal region, residues from 214 to 318 of VP2 or VP3, is involved in interactions with the VP1 pentamers, which has been demonstrated previously (Chen et al., 1998). It is not clear if phosphorylation in this region is involved in this interaction. However, the function of phosphorylation of the minor capsid proteins needs to be further investigated.

The structural proteins, VP1, VP2, and VP3, of BKV were highly modified with oxidation. Oxidative modification is frequently associated with aged or damaged proteins (Finkel and Holbrook, 2000).

Table 4
Summary and comparison of the modifications of BK VP2 and VP3 as identified by LC-MS/MS.

VP2 a.a. no.	a.a.[a]	Modification[b]	VP3 a.a. no.	a.a.[a]	Modification[b]
92	S	formylation	–	–	–
105	W	oxidation, dioxidation	–	–	–
120	M	oxidation	1	M	acetylation
148	D	x	30	D	oxidation
151	H	x	33	H	oxidation
153	W	oxidation	34	W	oxidation, dioxidation
166	W	oxidation	47	W	oxidation
167	H	x	48	H	oxidation
174	P	dioxidation	55	P	x
175	S	formylation	56	S	formylation
202	W	oxidation, dioxidation	83	W	oxidation, dioxidation
203	T	x	84	T	formylation
223	S	phosphorylation	104	S	x
227	P	oxidation, dioxidation	108	P	x
229	M	oxidation	110	M	oxidation
242	H	oxidation	123	H	oxidation
245	H	oxidation	126	H	oxidation
247	Y	oxidation	128	Y	oxidation
248	S	phosphorylation, formylation	129	S	phosphorylation, formylation
254	S	phosphorylation	135	S	formylation
259	T	formylation	140	T	formylation
262	M	oxidation, dioxidation	143	M	oxidation
269	S	formylation	150	S	formylation
271	H	x	152	H	oxidation
272	S	formylation	153	S	formylation
275	F	oxidation, dioxidation	156	F	oxidation, dioxidation
278	K	carboxymethylation	159	K	carboxymethylation
279	T	formylation	160	T	formylation
289	T	x	170	T	formylation
291	P	oxidation	172	P	x
293	W	oxidation	174	W	oxidation, dioxidation
294	M	oxidation, dioxidation	175	M	oxidation, dioxidation
296	P	dioxidation	177	P	x
304	T	formylation	185	T	formylation
319	K	x	200	K	carboxymethylation, formylation
339	K	x	220	K	formylation

x: no modification was found on such residue.
[a] Abbreviation of amino acid.
[b] Modification identified by LC-MS/MS.

Chaperons, heat shock proteins (HSPs), are important mediators in the sequestering and repair of proteins damaged in this way (Ruddock and Klappa, 1999). Recently, it has been demonstrated that SV40 VP1 is associated with HSP70 (Li et al., 2009) and it has been suggested that this is important for viral protein folding and assembly. However, the biological significance of the oxidative modification of the viral structural proteins needs to be further investigated.

Lysine is the only amino acid with carboxymethylation among the BK structural proteins. Protein carboxymethylation may be caused by various carboxy methyltransferases and modification usually can occur with glutamate, aspartic acid, and cysteine (Clarke et al., 1988). Carboxymethylation on lysine is usually preceded by non-enzymatic glycation and oxidation via a Millard reaction to generate a major advanced glycation end product (AGE; Vlassara et al., 1994). In addition, modification by carboxymethylation may also cause a net charge change to the polypeptide. Therefore, this modification is considered to be a potential modulator in chemotaxis (Hackett and Campochiaro, 1988), neurosecretory regulation (Diliberto et al., 1976), and diabetes metabolism (Curtiss and Witztum, 1985). However, more information is needed to understand the function(s) of carboxymethylation of the BK structural proteins.

Methylation of polyoma VP1 has been previously reported (Burton and Consigli, 1996). In this study, methylation was identified on Cys-10 of BK VP1. Acetylation has also been detected on the tyrosine residue of polyoma VP1 (Bolen et al., 1981); nonetheless, in our study, it was identified on the methionine of BK VP3. N-terminal acetylation is one of the most common modifications in eukaryotes (Bradshaw et al., 1998). The biological importance of N-terminal acetylation is well recognized. It may affect enzymatic activity, protein stability, DNA binding, protein–protein interactions, and receptor recognition (Starheim et al., 2009). Elucidation of the role of methionine acetylation of VP3 in the BKV life cycle will be of value. Other previously reported modifications, such as sulfation (Ludlow and Consigli, 1987b) and hydroxylation (Ludlow and Consigli, 1989), which have been found on polyoma VP1, were not detected for BK VP1 during this study. It is not clear whether these modification differences across the structural proteins of the polyomaviruses may result in different protein characteristics.

In conclusion, the viral proteins of BK were comprehensively analyzed. The characteristics of the BK structural proteins that have been revealed in this study may provide new insights into their interactions with the host cells during the viral life cycle.

Materials and methods

Virus propagation

Vero cells obtained from the American Type Culture Collection (ATCC; Manassas, VA, USA) were cultured in Eagle's Minimal Essential Medium (EMEM; Invitrogen, Grand Island, NY, USA) supplemented with 10% heat inactivated fetal bovine serum (FBS; Biological Industries, Beit Haemek, Israel) and 1% penicillin/streptomycin (P/S; Invitrogen). Cells were maintained at 37 °C in a humidified chamber with 5% CO_2. Cells were grown to 70% confluence before being infected with the virus. BKV (UT strain, a gift from Dr. W. Atwood), which had 4096 hemagglutination units (HAUs), was diluted in 2% FBS EMEM in a volume sufficient to cover the Vero cells. The virus was allowed to adsorb to the cells for 1.5 h at 37 °C with occasional tilting. Complete medium was then added, and the mixture was incubated at 37 °C with 5% CO_2 in a humidified incubator. Fresh medium was added to the infected cells once a week. After 4 weeks, when cytopathic effects were evident, infected cells were scraped off from the culture dishes. The cell lysate was then centrifuged at 1500×*g* for 15 min at 4 °C. The pellet containing the cell debris was used as the source of virus for purification.

Virus purification

The BKV-infected cell pellet was suspended in Tris-buffered saline (TBS, 10 mM Tris–HCl and 150 mM NaCl, pH 7.4). The cell debris was then subjected to three cycles of freezing and thawing at −80 °C and 37 °C, each for 1 h, with vortexing. The virus was then released by incubation with Type V neuraminidase (0.05 mg/ml; Sigma, St. Louis, MO, USA) at 37 °C for 16 h, followed by incubation at 56 °C for 30 min. The cell debris was removed by centrifugation at 3000×*g* and 4 °C for 30 min. The virus-containing supernatant was stored at 4 °C. The virus was then concentrated using a 20% sucrose cushion in TBS with centrifugation at 40,000 rpm for 1 h with an SW55.1 rotor (Beckman Coulter, Fullerton, CA, USA). The concentrated virus was resuspended and further centrifuged on a premade CsCl step gradient (1.35, 1.32, 1.29, 1.26, 1.23 g/ml) in an SW55.1 rotor (Beckman Coulter) at 35,000 rpm for 16 h at 4 °C. Thirty-three fractions were collected from the bottom of the tube. Each fraction was analyzed to determine its hemagglutination activity (HA) and the presence of viral proteins. The fractions containing HA were pooled together and dialyzed against TBS. The virus was then further concentrated using an Amicon® Ultra-15 concentrator (Millipore, Billerica, MA, USA).

Electron microscopy

In total, 5 μl (1 μg/μl) of purified BKV was loaded on a grid coated with perforated carbon film. The excess fluid was absorbed by a filter paper from the edge of the grid. Negative staining was performed with 2% uranyl acetate for 18 s. The specimen was observed under a Joel 2000-CX electron microscope operating at 120 kV.

Two-dimensional (2-D) gel electrophoresis

In total, 100 μl of rehydration buffer (7 M urea, 2 M thiourea, 4% CHAPS, 0.5% immobilized pH gradient (IPG) buffer, 90 mM dithrioerythritol (DTE), and 0.002% bromophenol blue) was added to the TCA precipitated viral proteins. Following incubation overnight (O/N) at 30 °C with occasional vortexing, the insoluble debris was removed by centrifugation at 15,000 × *g* at 15 °C for 5 min. Next, 18 cm IPG DryStrips created for pH 4–7 or 6–9 (Amersham Biosciences, Little Chalfont, Bucks, UK) were reswollen O/N at RT in 350 μl of rehydration buffer under 5 ml DryStrip Cover Fluid (Amersham Biosciences). The protein sample (25 to 35 μg) was cup-loaded close to the anode of the IPG strip and focused in an Etten™ IPGphor (Amersham Biosciences). The IPG strip was run in a gradient mode with the voltage increased from 500 to 4000 V and then maintained at 8000 V until the power reached around 60 kV h.

After focusing, the IPG strip was briefly rinsed with distilled water and transferred to the second-dimension gel. Before the second electrophoresis, the IPG strip was equilibrated in 3 ml equilibration buffer (50 mM Tris, pH 8.8; 6 M urea, 30% glycerol, 2% SDS, 0.002% bromophenol blue, and 130 mM DTE) for 15 min, followed by incubation for 15 min in the same solution, but this time containing 135 mM iodoacetamide (IAA) instead of DTE. The second-dimensional gel electrophoresis was performed using a 10% or 12.5% separating gel (18 cm × 18 cm × 1.5 mm) and a 4% stacking gel (1 cm × 18 cm × 1.5 mm) in PROTEAN II xi system (Bio-Rad, Hercules, CA, USA). The strip was transferred to the top of the gel and embedded in 0.5% agarose made up in Tris-glycine running buffer. The SDS-PAGE was run at 10 mA per IPG gel for 30 min and then separated at 40 mA per gel for 5.5 h.

Western blotting

Initially, the purified virus was resolved by 15% SDS-PAGE. The viral proteins were then transferred to a polyvinylidene fluoride (PVDF) membrane (Pall, East Hills, NY, USA) using a semi-dry electroblotting system (Thermo Fisher Scientific, Waltham, MA, USA) at 2.5 mA/cm^2 for 45 min. Polyclonal antibodies generated in rabbits against recombinant BK VP1 and VP2/3 were used to identify the VP1 and VP2/3 proteins. Viral histones were detected using anti-histone H2A, H2B, H3, and H4 (Upstate, Lake Placid, NY, USA) or H1 (Santa Cruz Biotechnology, Santa Cruz, CA, USA) antibodies. Bands were detected using an anti-IgG polyclonal antibody conjugated to peroxidase (Santa Cruz Biotechnology), followed by exposure to a chemiluminescent substrate (PerkinElmer Life Sciences, Foster City, CA, USA) and BioMax MR film (PerkinElmer Life Sciences). Two-dimensional gel protein spots were analyzed using the PD Quest 2-D gel analysis software version 6.2 (Bio-Rad). To identify valid spots, PD Quest spot detection software was employed for the appropriate selection of the faintest and the smallest spots in a large representative section of the image. Background and vertical streaks were removed from each gel image.

In-gel digestion

Protein bands from the SDS-PAGE or protein spots from 2-D gel were manually excised from the gel. The gel was diced in a siliconized centrifuge tube. The pieces of gel were then reduced with 50 mM DTE in 25 mM ammonium bicarbonate (pH 8.5) at 50 °C for 1 h. They were then alkylated with 100 mM IAA in 25 mM ammonium bicarbonate at RT for 1 h in the dark. The reduced and alkylated gel pieces were then washed twice in 50% acetonitrile in 25 mM ammonium bicarbonate and then vacuum dried. Gel pieces were rehydrated with solution containing sequencing-grade trypsin, chymotrypsin, or GluC (Thermo Fisher Scientific, 20 μg/ml in 25 mM ammonium bicarbonate, pH 8.5) at 37 °C for 4 h. Following enzyme digestion, the tryptic peptides were extracted three times using 50% acetonitrile in 5% formic acid for 15 min each time. The extracted solution was pooled together and dried by Speed-Vac.

Nano-LC-MS/MS analysis

High resolution and high mass accuracy nanoflow LC-MS/MS was performed on an LTQ-FT (Linear quadrupole ion trap-Fourier transform ion cyclotron resonance) mass spectrometer (Thermo Fisher Scientific) that was equipped with a nanoelectrospray ion source (New Objective, Woburn, MA, USA), an Agilent 1100 Series binary high-performance liquid chromatography pump (Agilent Technologies, Palo Alto, CA, USA), and a Famos autosampler (LC Packings, San Francisco, CA, USA). The digested peptide solution was injected onto a self-packed precolumn (150 μm I.D. × 20 mm, 5 μm, 200 Å). Chromatographic separation was performed on a self-packed reversed phase C18 nanocolumn (75 μm I.D. × 150 mm, 5 μm, 100 Å) using 0.1% formic acid in water (mobile phase A) and 0.1% formic acid in 80% acetonitrile (mobile phase B). This was done by applying a linear gradient from 5% to 40% mobile phase B for 40 min at a flow rate of 300 nl/min; this was provided across a flow splitter by the HPLC pumps. Electrospray voltage was applied at 2 kV and capillary temperature was set at 200 °C.

A scan cycle was initiated using a full-scan survey MS spectrum (m/z 300–2000); this was performed on the FT-ICR mass spectrometer with a resolution of 100,000 (at m/z 400). The 10 most abundant ions detected in this scan were subjected to an MS/MS experiment performed in the linear quadrupole ion trap (LTQ) mass spectrometer. Ion accumulation (Auto Gain Control target number) and maximal ion accumulation time for full-scan and MS/MS modes were set at 1×10^6 ions, 1000 ms and 5×10^4 ions, 200 ms, respectively. The parameters of the collision-induced dissociation (CID) were given as follows: the normalized collision energy was set to 35%, while the activation *Q* was set at 0.3 and the activation time was 30 ms.

For data analysis, all MS/MS spectra were converted into the DTA format from the experiment RAW file by Bioworks (Thermo Fisher Scientific) then merged into a single file for Mascot (ver. 2.2, Matrix Science, Boston, MA, USA) MS/MS ion search. The precursor ion error tolerance and fragment ion error tolerance in MS/MS were set at 10 ppm and 0.6 Da, respectively. The miscleavage number for the enzyme digestion was set to three. Protein post-translational modifications, such as methione oxidation, lysine/arginine methylation, lysine acetylation, serine/tyrosine/threonine phosphorylation, and cysteine carboxyamidomethylation, were assigned in the data search as part of Mascot analysis.

Acknowledgments

We would like to thank Dr. W. Atwood for kindly giving us the BK virus. This work was supported by the National Science Council Grant NSC97-2320-B-194-001-MY3, Taiwan.

Appendix A. Supplementary data

Supplementary data associated with this article can be found, in the online version, at doi:10.1016/j.virol.2010.03.029.

References

Allander, T., Andreasson, K., Gupta, S., Bjerkner, A., Bogdanovic, G., Persson, M.A., Dalianis, T., Ramqvist, T., Andersson, B., 2007. Identification of a third human polyomavirus. J. Virol. 81 (8), 4130–4136.

Anders, D.G., Consigli, R.A., 1983. Comparison of nonphosphorylated and phosphorylated species of polyomavirus major capsid protein VP1 and identification of the major phosphorylation region. J. Virol. 48 (1), 206–217.

Barban, S., 1973. Electrophoretic differences in the capsid proteins of simian virus 40 plaque mutants. J. Virol. 11 (6), 971–977.
Barbanti-Brodano, G., Lambertini, L., Tampirei, M., Minelli, G.P., Portolani, M., Zerbini, M., 1976. Differences between BK virus and simian virus 40 structural proteins analysed by isoelectric focusing. Arch. Virol. 51 (1–2), 163–167.
Boldorini, R., Allegrini, S., Miglio, U., Paganotti, A., Veggiani, C., Mischitelli, M., Monga, G., Pietropaolo, V., 2009. Genomic mutations of viral protein 1 and BK virus nephropathy in kidney transplant recipients. J. Med. Virol. 81 (8), 1385–1393.
Bolen, J.B., Consigli, R.A., 1979. Differential adsorption of polyoma virions and capsids to mouse kidney cells and guinea pig erythrocytes. J. Virol. 32 (2), 679–683.
Bolen, J.B., Anders, D.G., Trempy, J., Consigli, R.A., 1981. Differences in the subpopulations of the structural proteins of polyoma virions and capsids: biological functions of the multiple VP1 species. J. Virol. 37 (1), 80–91.
Bradshaw, R.A., Brickey, W.W., Walker, K.W., 1998. N-terminal processing: the methionine aminopeptidase and N alpha-acetyl transferase families. Trends Biochem. Sci. 23 (7), 263–267.
Burton, K.S., Consigli, R.A., 1996. Methylation of the polyomavirus major capsid protein VP1. Virus Res. 40 (2), 141–147.
Chen, X.S., Stehle, T., Harrison, S.C., 1998. Interaction of polyomavirus internal protein VP2 with the major capsid protein VP1 and implications for participation of VP2 in viral entry. EMBO J. 17 (12), 3233–3240.
Chen, P.L., Wang, M., Ou, W.C., Lii, C.K., Chen, L.S., Chang, D., 2001. Disulfide bonds stabilize JC virus capsid-like structure by protecting calcium ions from chelation. FEBS Lett. 500 (3), 109–113.
Clarke, S., Vogel, J.P., Deschenes, R.J., Stock, J., 1988. Posttranslational modification of the Ha-ras oncogene protein: evidence for a third class of protein carboxyl methyltransferases. Proc. Natl. Acad. Sci. U. S. A. 85 (13), 4643–4647.
Curtiss, L.K., Witztum, J.L., 1985. Plasma apolipoproteins AI, AII, B, CI, and E are glucosylated in hyperglycemic diabetic subjects. Diabetes 34 (5), 452–461.
Daniels, R., Rusan, N.M., Wadsworth, P., Hebert, D.N., 2006. SV40 VP2 and VP3 insertion into ER membranes is controlled by the capsid protein VP1: implications for DNA translocation out of the ER. Mol. Cell 24 (6), 955–966.
Diliberto Jr., D.J., Veiveros, O.H., Axelrod, J., 1976. Subcellular distribution of protein carboxymethylase and its endogenous substrates in the adrenal medulla: possible role in excitation–secretion coupling. Proc. Natl. Acad. Sci. U. S. A. 73 (11), 4050–4054.
Feng, H., Shuda, M., Chang, Y., Moore, P.S., 2008. Clonal integration of a polyomavirus in human Merkel cell carcinoma. Science 319 (5866), 1096–1100.
Finkel, T., Holbrook, N.J., 2000. Oxidants, oxidative stress and the biology of ageing. Nature 408 (6809), 239–247.
Forstova, J., Krauzewicz, N., Wallace, S., Street, A.J., Dilworth, S.M., Beard, S., Griffin, B.E., 1993. Cooperation of structural proteins during late events in the life cycle of polyomavirus. J. Virol. 67 (3), 1405–1413.
Friedmann, T., 1976. Structural proteins of polyoma virus: proteolytic degradation of virion proteins by exogenous and by virion-associated proteases. J. Virol. 20 (2), 520–526.
Garcea, R.L., Ballmer-Hofer, K., Benjamin, T.L., 1985. Virion assembly defect of polyomavirus hr-t mutants: underphosphorylation of major capsid protein VP1 before viral DNA encapsidation. J. Virol. 54 (2), 311–316.
Gasparovic, M.L., Gee, G.V., Atwood, W.J., 2006. JC virus minor capsid proteins Vp2 and Vp3 are essential for virus propagation. J. Virol. 80 (21), 10858–10861.
Gaynor, A.M., Nissen, M.D., Whiley, D.M., Mackay, I.M., Lambert, S.B., Wu, G., Brennan, D.C., Storch, G.A., Sloots, T.P., Wang, D., 2007. Identification of a novel polyomavirus from patients with acute respiratory tract infections. PLoS Pathog. 3 (5), e64.
Gharakhanian, E., Munoz, L., Mayorca, L., 2003. The simian virus 40 minor structural protein Vp3, but not Vp2, is essential for infectious virion formation. J. Gen. Virol. 84 (Pt 8), 2111–2116.
Hackett, S.F., Campochiaro, P.A., 1988. Implication of protein carboxymethylationin retinal pigment epithelial cell chemotaxis. Ophthalmic Res. 20 (1), 54–59.
Haynes II, J.I., Consigli, R.A., 1992. Phosphorylation of the budgerigar fledgling disease virus major capsid protein VP1. J. Virol. 66 (7), 4551–4555.
Hewick, R.M., Waterfield, M.D., Miller, L.K., Fried, M., 1977. Correlation between genetic loci and structural differences in the capsid proteins of polyoma virus plaque morphology mutants. Cell 11 (2), 331–338.
Iida, T., Kitamura, T., Guo, J., Taguchi, F., Aso, Y., Nagashima, K., Yogo, Y., 1993. Origin of JC polyomavirus variants associated with progressive multifocal leukoencephalopathy. Proc. Natl. Acad. Sci. U. S. A. 90 (11), 5062–5065.
Krauzewicz, N., Streuli, C.H., Stuart-Smith, N., Jones, M.D., Wallace, S., Griffin, B.E., 1990. Myristylated polyomavirus VP2: role in the life cycle of the virus. J. Virol. 64 (9), 4414–4420.
Li, M., Garcea, R.L., 1994. Identification of the threonine phosphorylation sites on the polyomavirus major capsid protein VP1: relationship to the activity of middle T antigen. J. Virol. 68 (1), 320–327.
Li, M., Lyon, M.K., Garcea, R.L., 1995. In vitro phosphorylation of the polyomavirus major capsid protein VP1 on serine 66 by casein kinase II. J. Biol. Chem. 270 (43), 26006–26011.
Li, P.P., Itoh, N., Watanabe, M., Shi, Y., Liu, P., Yang, H.J., Kasamatsu, H., 2009. Association of simian virus 40 vp1 with 70-kilodalton heat shock proteins and viral tumor antigens. J. Virol. 83 (1), 37–46.
Liddington, R.C., Yan, Y., Moulai, J., Sahli, R., Benjamin, T.L., Harrison, S.C., 1991. Structure of simian virus 40 at 3.8-A resolution. Nature 354 (6351), 278–284.
Ludlow, J.W., Consigli, R.A., 1987a. Localization of calcium on the polyomavirus VP1 capsid protein. J. Virol. 61 (9), 2934–2937.
Ludlow, J.W., Consigli, R.A., 1987b. Polyomavirus major capsid protein VP1 is modified by tyrosine sulfuration. J. Virol. 61 (5), 1708–1711.
Ludlow, J.W., Consigli, R.A., 1989. Hydroxyproline in the major capsid protein VP1 of polyomavirus. J. Virol. 63 (6), 2881–2884.
O'Farrell, P.Z., Goodman, H.M., 1976. Resolution of simian virus 40 proteins in whole cell extracts by two-dimensional electrophoresis: heterogeneity of the major capsid protein. Cell 9 (2), 289–298.
Ou, W.C., Wang, M., Fung, C.Y., Tsai, R.T., Chao, P.C., Hseu, T.H., Chang, D., 1999. The major capsid protein, VP1, of human JC virus expressed in Escherichia coli is able to self-assemble into a capsid-like particle and deliver exogenous DNA into human kidney cells. J. Gen. Virol. 80 (Pt 1), 39–46.
Perez-Losada, M., Christensen, R.G., McClellan, D.A., Adams, B.J., Viscidi, R.P., Demma, J.C., Crandall, K.A., 2006. Comparing phylogenetic codivergence between polyomaviruses and their hosts. J. Virol. 80 (12), 5663–5669.
Ponder, B.A., Robbins, A.K., Crawford, L.V., 1977. Phosphorylation of polyoma and SV40 virus proteins. J. Gen. Virol. 37 (1), 75–83.
Rayment, I., Baker, T.S., Caspar, D.L., Murakami, W.T., 1982. Polyoma virus capsid structure at 22.5 A resolution. Nature 295 (5845), 110–115.
Ruddock, L.W., Klappa, P., 1999. Oxidative stress: protein folding with a novel redox switch. Curr. Biol. 9 (11), R400–R402.
Sahli, R., Freund, R., Dubensky, T., Garcea, R., Bronson, R., Benjamin, T., 1993. Defect in entry and altered pathogenicity of a polyoma virus mutant blocked in VP2 myristylation. Virology 192 (1), 142–153.
Salunke, D.M., Caspar, D.L., Garcea, R.L., 1986. Self-assembly of purified polyomavirus capsid protein VP1. Cell 46 (6), 895–904.
Schmidt, M., Muller, H., Schmidt, M.F., Rott, R., 1989. Myristoylation of budgerigar fledgling disease virus capsid protein VP2. J. Virol. 63 (1), 429–431.
Starheim, K.K., Gromyko, D., Velde, R., Varhaug, J.E., Arnesen, T., 2009. Composition and biological significance of the human N alpha-terminal acetyltransferases. BMC Proc. 3 (Suppl 6), S3.
Stehle, T., Yan, Y., Benjamin, T.L., Harrison, S.C., 1994. Structure of murine polyomavirus complexed with an oligosaccharide receptor fragment. Nature 369 (6476), 160–163.
Streuli, C.H., Griffin, B.E., 1987. Myristic acid is coupled to a structural protein of polyoma virus and SV40. Nature 326 (6113), 619–622.
Tan, K.B., Sokol, F., 1972. Structural proteins of simian virus 40: phosphoproteins. J. Virol. 10 (5), 985–994.
Tooze, J., 1981. Molecular biology of tumor viruses. Part 2. DNA tumor viruses, 2nd ed. Cold Spring Harbor Laboratory, New York.
Vlassara, H., Bucala, R., Striker, L., 1994. Pathogenic effects of advanced glycosylation: biochemical, biologic, and clinical implications for diabetes and aging. Lab. Invest. 70 (2), 138–151.
Zheng, H.Y., Ikegaya, H., Takasaka, T., Matsushima-Ohno, T., Sakurai, M., Kanazawa, I., Kishida, S., Nagashima, K., Kitamura, T., Yogo, Y., 2005. Characterization of the VP1 loop mutations widespread among JC polyomavirus isolates associated with progressive multifocal leukoencephalopathy. Biochem. Biophys. Res. Commun. 333 (3), 996–1002.